Lithium Increases Synapse Formation between Hippocampal Neurons by Depleting Phosphoinositides[S]

Hee Jung Kim and Stanley A. Thayer

Department of Pharmacology, University of Minnesota Medical School, Minneapolis, Minnesota

Received September 29, 2008; accepted February 2, 2009

ABSTRACT

The mood-stabilizing effects of lithium are well documented, although its mechanism of action remains unknown. Increases in gray matter volume detected in patients with bipolar disorder who were treated with lithium suggest that changes in the number of synapses might underlie its therapeutic effects. We investigated the effects of lithium on the number of synaptic connections between hippocampal neurons in culture. Confocal imaging of neurons expressing postsynaptic density protein 95 fused to green fluorescent protein (PSD95-GFP) enabled visualization of synaptic sites. PSD95-GFP fluorescent puncta represented functional synapses, and lithium (4 h, 5 mM) increased their number by $150 \pm 12\%$. The increase was time- and concentration-dependent ($EC_{50} = 1.0 \pm 0.6$ mM). Lithium induced a parallel increase in the presynaptic marker synaptophysin-GFP. Valproic acid, another mood stabilizer, also increased the number of fluorescent puncta at a clinically relevant concentration. Inhibi-

tion of postsynaptic glutamate receptors or presynaptic inhibition of neurotransmitter release significantly reduced lithium-induced synapse formation, indicating that glutamatergic synaptic transmission was required. Pretreatment with exogenous myo-inositol inhibited synapse formation, demonstrating that depletion of inositol was necessary to increase synaptic connections. In contrast, inhibition of glycogen synthase kinase 3β did not mimic lithium-induced synapse formation. Pharmacological and lipid reconstitution experiments showed that new synapses formed as a result of depletion of phosphatidylinositol-4-phosphate rather than a build-up of polyphosphoinositides or changes in the activity of phospholipase C, protein kinase C, or phosphatidylinositol-3-kinase. Increased synaptic connections may underlie the mood-stabilizing effects of lithium in patients with bipolar disorder and could contribute to the convulsions produced by excessive doses of this drug.

Lithium has been used to treat bipolar disorder for decades, yet its mechanism of therapeutic action remains unknown. Lithium exerts a number of powerful effects on neuronal signaling pathways (Schloesser et al., 2008): it displays neuroprotective and neurotrophic properties (Chuang and Manji, 2007);

it induces axonal sprouting (Hall et al., 2000); and long-term lithium treatment increases neurogenesis (Chen et al., 2000). The contributions of these effects to the stabilization of mood or the untoward effects of lithium are unclear. In this context, it is noteworthy that brain-imaging studies have detected increased gray matter volumes in patients with bipolar disorder after long-term administration of lithium (Chen et al., 2000; Sassi et al., 2002). This increase might be associated with an increase in the volume of the neuropil, suggesting that lithium may enhance synaptic connections.

Lithium acts on two molecular targets that might increase synapse formation at therapeutically relevant concentra-

ABBREVIATIONS: IMPase, inositol monophosphatase; IPPase, inositol polyphosphate 1-phosphatase; PSD95, postsynaptic density protein 95; GFP, green fluorescent protein; PSD95-GFP, postsynaptic density protein 95 fused to green fluorescent protein; PtdIns(4)P, phosphatidylinositol-4-phosphate; PtdIns(4,5)P_2, phosphatidylinositol-4,5-phosphate; GSK-3β, glycogen synthase kinase-3β; NMDA, N-methyl-D-aspartate; MK801, dizocilpine; DMEM, Dulbecco's modified Eagle's medium; HHSS, HEPES-buffered Hanks' salt solution; PI3K, phosphatidylinositol 3-kinase; PLC, phospholipase C; FAK, focal adhesion kinase; FM4−64FX, fixable version of N-(3-triethylammoniumpropyl)-4-(6-(4-(diethylamino)phenyl)hexatrienyl)pyridinium dibromide; PKC, protein kinase C; ANOVA, analysis of variance; CNQX, 6-cyano-2,3-dihydroxy-7-nitroquinoxaline; L803-mts, N-myristol-GKEAPPAPPQS(p)P; SB216763, 3-(2,4-dichlorophenyl)-4-(1-methyl-1H-indol-3-yl)-1H-pyrrole-2,5-dione; SB415286, 3-[(3-chloro-4-hydroxyphenyl)amino]-4-(2-nitrophenyl)-1H-pyrrol-2,5-dione; U73122, 1-[6-[[17β-methoxyestra-1,3,5(10)-trien-17-yl]amino]hexyl]-1H-pyrrole-2,5-dione; Gö6976, 12-(2-cyanoethyl)-6,7,12,13-tetrahydro-13-methyl-5-oxo-5H-indolo(2,3-a)pyrrolo(3,4-c)-carbazole; Ro-31-8220, 3-1-[3-(amidinothio)propyl-1H-indol-3-yl]-3-(1-methyl-1H-indol-3-yl) maleimide (bisindolylmaleimide IX); Win 55,212-2, (R)-(+)-[2,3-dihydro-5-methyl-3-[(4-morpholinyl)methyl] pyrrolo-[1,2,3-de]-1,4-benzoxazin-6-yl](1-napthalenyl)methanone monomethanesulfonate; XE991, 10,10-bis(4-pyridinylmethyl)-9(10H)-anthracenone.

tions. Lithium depletes brain inositol levels in rats by in-hibiting inositol monophosphatase (IMPase) and inositol polyphosphate 1-phosphatase (IPPase) (Allison and Stewart, 1971). Complete inhibition of IMPase could deplete phospha-tidylinositol-4-phosphate [PtdIns(4)P], $PtdIns(4,5)P_2$, elimi-nate inositol triphosphate signaling, and increase the levels of inositol monophosphates (Berridge, 1989). Lithium-in-duced depletion of inositol increased the spread and reduced the collapse of neuronal growth cones, events linked to syn-apse formation (Williams et al., 2002). Inhibition of glycogen synthase kinase-3β (GSK-3β) may account for the prolifera-tive and antiapoptotic effects of lithium (Wexler et al., 2008). Lithium mimics activation of the Wnt signaling pathway, which initiates the axonal remodeling that is an early event in synapse formation (Hall et al., 2000). GSK-3β phosphory-lates the microtubule-associated protein τ, and thus, its in-hibition could account for some of the neuroprotective effects of lithium, including preservation of synaptic density (Love-stone et al., 1999). Other potential sites of action for mood stabilizers with a less clear link to stimulating new synapse formation include inhibition of the arachidonic acid cascade, inhibition of protein kinase C, and inhibition of adenylyl cyclase (Gould et al., 2004).

Recent advances in imaging techniques make it possible to follow the assembly of synapses in living cells (Friedman et al., 2000; Okabe et al., 2001). Synapse formation is a dynamic process, and the formation of functional synapses can occur rapidly over the course of a few hours. Postsynaptic density protein 95 (PSD95) is a scaffolding protein that anchors receptors, including the NMDA receptor, and downstream signaling molecules to the postsynaptic density (Kim and Sheng, 2004). Presynaptic differentiation precedes a gradual recruitment of PSD95 to newly formed synaptic sites (Fried-man et al., 2000). Thus, PSD95 is widely used as a marker for synapses (Okabe et al., 1999). We developed an imaging-based assay that tracks green fluorescent puncta that form in the dendrites of cells expressing PSD95 fused to green fluo-rescent protein (PSD95-GFP) (Waataja et al., 2008).

Here, we used this assay to quantify changes in the num-ber of synapses between hippocampal neurons over time. We show that lithium induced the formation of synapses between hippocampal neurons in culture. We tested the hypothesis that lithium induces synapse formation via inositol depletion and subsequent down-regulation of the phosphoinositide sig-naling cascade.

Materials and Methods

Materials. Materials were obtained from the following sources: PSD95-GFP expression vector (pGW1-CMV-PSD-95:GFP) was kindly provided by Donald B. Arnold (University of Southern California, Los Angeles, CA); synaptophysin-GFP expression vector (pSynaptophysin-EGFPN1) was kindly provided by Jane Sullivan (University of Wash-ington, Seattle, WA); expression vector for DsRed2 (pDsRed2-N1) was from Clontech (Mountain View, CA); Dulbecco's modified Eagle's me-dium (DMEM), fetal bovine serum, and horse serum were from Invitro-gen (Carlsbad, CA); D-*myo*-phosphatidylinositol 4-phosphate was from Echelon Biosciences Incorporated (Salt Lake City, UT); and cyclohexi-mide, dizocilpine (MK801), and all other reagents were from Sigma (St. Louis, MO).

Lipid Delivery. PtdIns(4)P was delivered via the Shuttle PIP system (Echelon Biosciences) (Ozaki et al., 2000). PtdIns(4)P diC_{16} was freshly prepared at a concentration of 400 μM in 150 mM NaCl,

4 mM KCl, and 20 mM HEPES at pH 7.2. PtdIns(4)P-carrier 3 complex was prepared by mixing phospholipids with an equal vol-ume of 400 μM freshly prepared carrier 3, vortexed vigorously, incubated for 10 min at room temperature, and then diluted 1:4 with DMEM immediately before addition to the culture.

Cell Culture. Rat hippocampal neurons were grown in primary culture as described previously (Shen et al., 1996) with minor mod-ifications. Fetuses were removed on embryonic day 17 from maternal rats euthanized by CO_2 inhalation. Hippocampi were dissected and placed in Ca^{2+}- and Mg^{2+}-free HEPES-buffered Hanks' salt solution (HHSS), pH 7.45. HHSS was composed of 20 mM HEPES, 137 mM NaCl, 1.3 mM $CaCl_2$, 0.4 mM $MgSO_4$, 0.5 mM $MgCl_2$, 5.0 mM KCl, 0.4 mM KH_2PO_4, 0.6 mM Na_2HPO_4, 3.0 mM $NaHCO_3$, and 5.6 mM glucose. Cells were dissociated by trituration through a 5-ml pipette and a flame-narrowed Pasteur pipette, pelleted, and resuspended in DMEM without glutamine, supplemented with 10% fetal bovine serum and penicillin/streptomycin (100 U/ml and 100 μg/ml, respec-tively). Dissociated cells were then plated at a density of 10,000 to 20,000 cells/dish onto a 25-mm round cover glass (no. 1) glued to cover a 19-mm diameter opening drilled through the bottom of a 35-mm Petri dish. The coverglass was precoated with Matrigel (200 μl, 0.2 mg/ml; BD Bioscience, San Jose, CA). Neurons were grown in a humidified atmosphere of 10% CO_2 and 90% air, pH 7.4, at 37°C, and fed on days 1 and 6 by an exchange of 75% of the media with DMEM, supplemented with 10% horse serum and penicillin/strepto-mycin. Cells were cultured without mitotic inhibitors for a minimum of 12 days, at which point they formed functional synapses and displayed spontaneous network activity (Kim et al., 2008; Waataja et al., 2008).

Transfection. Rat hippocampal neurons were transfected after 10 to 13 days in vitro using a modification of a protocol described previously (Waataja et al., 2008). In brief, hippocampal cultures were incubated for at least 20 min in DMEM supplemented with 1 mM kynurenic acid, 10 mM $MgCl_2$, and 5 mM HEPES to reduce neuro-toxicity. A DNA/calcium phosphate precipitate containing 1 μg of DNA of each plasmid per well was prepared, allowed to form for 30 min at room temperature, and added to the culture. After a 90-min incubation, cells were washed once with DMEM supplemented with $MgCl_2$ and HEPES and then returned to conditioned media, which was saved at the beginning of the procedure.

Confocal Imaging. Transfected neurons were transferred to the stage of a confocal microscope (Fluoview 300; Olympus, Melville, NY) and viewed through a 60× oil-immersion objective (numerical aper-ture, 1.40). For experiments in which the same neurons were imaged before and after a 4-h interval, the locations of individual cells were recorded using micrometers attached to the stage of the microscope. Multiple optical sections spanning 8 μm in the *z*-dimension were collected (1-μm steps) and combined through the *z*-axis into a com-pressed *z* stack. GFP was excited at 488 nm with an argon ion laser and emission was collected at 530 nm (10 nm bandpass). The exci-tation and emission wavelengths for DsRed2 were 543 nm (green HeNe laser) and >605 nm, respectively.

Image Processing. To count and label PSD95-GFP puncta, an automated algorithm was created using MetaMorph 6.2 image pro-cessing software described previously (Waataja et al., 2008). In brief, maximum *z*-projection images were created from the DsRed2 and GFP image stacks. Next, a threshold set 1 S.D. above the image mean was applied to the DsRed2 image. This created a 1-bit image that was used as a mask via a logical AND function with the GFP maximum *z*-projection. A top-hat filter (80 pixels) was applied to the masked PSD95-GFP image. A threshold set 1.5 S.D. above the mean intensity inside the mask was then applied to the contrast enhanced image. Structures between 8 and 80 pixels were counted as PSDs. The structures were then dilated and superimposed on the DsRed2 maximum *z*-projection for visualization. PSD counts were presented as mean $\pm$ S.E.M., where *n* is the number of cells, each from separate cover glass over multiple cultures. We used Student's two-tailed *t*

test for single or ANOVA with Bonferroni's post test for multiple statistical comparisons.

Immunocytochemistry. Rat hippocampal neurons were labeled using a protocol described previously (Kim et al., 2008). In brief, PSD95-GFP-transfected hippocampal neurons were fixed with cooled methanol for 10 min at −20°C, blocked with 10% bovine serum albumin, and incubated for 16 h at 4°C with the following primary antibodies: mouse anti-NR2A (1:200; Chemicon, Temecula, CA), mouse anti-NR2B (1:200; Transduction Laboratories, Lexington, KY), and rabbit anti-DsRed (1:100; Clontech). Cells were then incubated in tetramethylrhodamine isothiocyanate-labeled anti-rabbit antiserum (Dako Denmark A/S, Glostrup, Denmark) and Alexa Fluor 647 anti-mouse IgG (Invitrogen) for 1 h at room temperature. After washing in phosphate-buffered saline, coverslips were inverted on slides over a drop of Fluoromount-G (Southern Biotechnology Associates, Birmingham, AL). GFP (excitation, 488 nm; emission, 530 nm; 10-nm bandpass), tetramethylrhodamine isothiocyanate (excitation, 543 nm; emission, >605 nm), and Alexa Fluor 647 (excitation, 633 nm; emission, >645 nm) -labeled neurons were imaged using confocal microscopy.

FM4–64FX Labeling. To label functional neurotransmitter release sites, hippocampal neurons expressing PSD95-GFP were loaded with FM4–64FX [fixable version of *N*-(3-triethylammonium-propyl)-4-(6-(4-(diethylamino)phenyl)hexatrienyl)pyridinium dibromide] (Invitrogen) as described previously (Waataja et al., 2008) with minor modifications. Cells were incubated in HHSS containing 50 mM K^+ (K^+ was exchanged reciprocally for Na^+) containing 10 μM FM4–64FX, 10 μM MK801, and 10 μM CNQX for 2 min. Excess dye was removed by incubating for 10 min in HHSS containing 500 μM Advasep-7, 10 μM MK801, and 10 μM CNQX. Neurons were then fixed in 4% paraformaldehyde/0.2% glutaraldehyde containing 4% sucrose in phosphate-buffered saline for 10 min. After washing in phosphate-buffered saline, coverslips were inverted on slides over a drop of Fluoromount-G and imaged using confocal microscopy (excitation, 543 nm; emission, >605 nm).

Results

Lithium Induces Synapse Formation. We have described previously a method to track changes in the number of postsynaptic sites visualized by confocal imaging of hippocampal neurons expressing PSD95-GFP and DsRed2 (Kim et al., 2008; Waataja et al., 2008). In Fig. 1A, we show representative images of rat hippocampal neurons in culture 48 h after transfection with expression plasmids for PSD95-GFP and DsRed2.
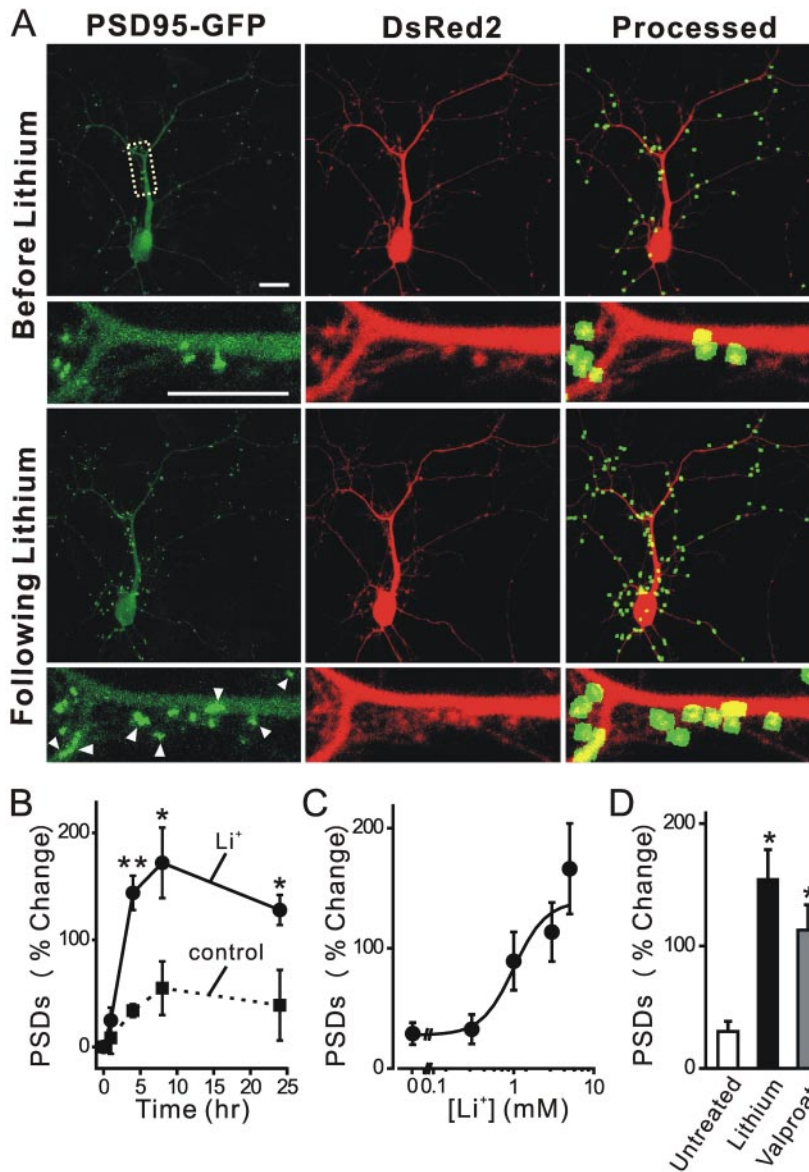

Fig. 1. Lithium induces synapse formation. A, confocal fluorescent images display maximum *z*-projections of a neuron expressing PSD95-GFP and DsRed2 before and 4 h after treatment with 5 mM lithium. Processing of PSD95-GFP images identified PSDs as fluorescent puncta meeting intensity and size criteria and in contact with a mask derived from the DsRed2 image. Labeled PSDs were dilated and overlaid on the DsRed2 image for viewing purposes (processed). Counting preceded dilation and labeling, so PSDs in close proximity were counted individually. The insets are enlarged images of the boxed region. Scale bar, 10 μm. B and C, lithium-induced synapse formation is time- and concentration-dependent. B, the number of PSDs increased after application of 5 mM lithium (●, solid line) at time 0. The number of PSDs seemed to increase under control conditions (■, broken line), but this trend was not significantly different ($p = 0.41$ ANOVA) from the starting value (t = 0). C, PSD formation depended on the concentration of lithium. Neurons expressing PSD95-GFP and DsRed2 were imaged before and after 4-h exposure to the indicated concentration of lithium (for each concentration, $n \geq 6$). The curve was fit by a logistic equation of the form % PSD change = $[(A_2 - A_1)/(1 + (X/EC_{50})^{nH})] + A_1$, where X = lithium concentration, A_1 = 28 ± 11% PSD change observed without the addition of lithium, A_2 = percentage of PSD change observed at the maximally effective lithium concentration, and n_H = slope factor. EC_{50} values were calculated using a nonlinear, least-squares curve-fitting program (Origin 6.0, OriginLab Corp, Northampton, MA) and are expressed as mean ± S.E.M. EC_{50}, A_2, and n_H were 1.0 ± 0.6 mM, 139 ± 39%, and 2.2 ± 2.2, respectively. D, valproate induces synapse formation. Bar graph summarizes the effects of mood stabilizers including lithium (5 mM), valproate (1 mM), and carbamazepine (50 μM, CBZ) on changes in the number of PSD95-GFP puncta (PSDs) after 4 h of treatment. Data are expressed as mean ± S.E.M. *, $p < 0.05$, **, $p < 0.01$, relative to untreated; ANOVA with Bonferroni post test.

PSD95-GFP expressed as discrete puncta that contrasted well from diffuse green fluorescence found throughout the cell. DsRed2 expression filled the soma and dendrites and was used to track morphological changes, as a mask for image processing, and to determine cell viability based on cytoplasmic retention of the fluorescent protein. Image processing identified and counted puncta by locating intensity peaks of the appropriate size (mean diameter, 0.52 μm) in contact with the DsRed2 mask. We demonstrated previously that fluorescent puncta identified by this image-processing algorithm colocalize with neurotransmitter release sites, NMDA-induced Ca^{2+} increases, and NMDA receptor immunoreactivity. Thus, PSD95-GFP puncta represent functional postsynaptic sites (Waataja et al., 2008).

We used this method to investigate the effects of lithium on the number of synaptic connections between hippocampal neurons in culture. Treatment with 5 mM lithium for 4 h increased the number of fluorescent puncta by $150 \pm 12\%$ ($n = 26$) (Fig. 1). The synaptic network is dynamic; after treatment with lithium, some existing puncta were lost, and many new puncta were formed, resulting in a net increase in the number of puncta. Because changes in neuronal morphology occurred over the course of the 4-h experiment, it is difficult to track individual synapses over time. This increase was significantly greater than that seen under control conditions ($38 \pm 7\%$; $n = 25$).

The time course for lithium-induced changes in the number of PSD95-GFP puncta is shown in Fig. 1B. A significant increase in the number of PSD95-GFP puncta was detected as early as 4 h after exposure to lithium ($144 \pm 16\%$, $p < 0.01$, $n = 6$). This observation is consistent with a previous study showing that individual glutamatergic synapses between cultured hippocampal neurons can form within 1 to 2 h (Friedman et al., 2000). The number of new synapses increased by $172 \pm 33\%$ by 8 h and was still elevated after 24 h ($128 \pm 14\%$, $p < 0.05$, $n = 5$). The number of PSD95-GFP puncta also increased in a graded fashion under control conditions, although the change was smaller ($55 \pm 25\%$ at 8 h, $n = 5$). In a previous study, we found that the formation of synapses under control conditions was triggered by the exchange of the media and required protein synthesis (blocked by cycloheximide), but it did not require synaptic activity (no effect of tetrodotoxin) (Kim et al., 2008). Lithium-induced synapse formation was concentration-dependent ($EC_{50} = 1.0 \pm 0.6$ mM) (Fig. 1C). The therapeutic concentration of extracellular lithium as reflected in the plasma of bipolar patients is in the range of 0.8 to 1.2 mM (Baldessarini and Tarazi, 2006), indicating that the synaptic effects described here occur at clinically relevant concentrations. The formation of new synapses described here is much faster than the therapeutic effects of lithium, which develop over several weeks (Baldessarini and Tarazi, 2006). Perhaps synapse formation is accelerated in this in vitro model, or maybe it represents an early change that contributes to the subsequent stabilization of mood.

We next compared the effects of lithium with the mood-stabilizing agents valproate and carbamazepine on synapse formation. The therapeutic concentration of valproate in the blood is as high as 0.7 mM (Baldessarini and Tarazi, 2006). As shown in Fig. 1D, valproate increased the number of PSDs at a therapeutically relevant concentration of 1 mM ($113 \pm 21\%$, $n = 7$). However, 50 μM carbamazepine, a concentration used clinically (Baldessarini and Tarazi, 2006), did not significantly affect the number of synapses ($59 \pm 11\%$, $n = 7$). Up-regulation of synapses may be a mechanism shared by agents that stabilize mood, although here we focus on the actions of lithium.

New PSD95-GFP Fluorescent Puncta Induced by Lithium Represent Synaptic Sites. Functional PSDs are composed of many proteins, including NMDA receptors. To determine whether the new PSD95-GFP puncta formed during treatment with lithium represent synaptic sites, we fixed neurons expressing PSD95-GFP and labeled them with antibodies to the NR2A and NR2B subunits of the NMDA receptor (Fig. 2A). Immunocytochemistry revealed that $69 \pm 3\%$ ($n = 5$) of PSD95-GFP puncta colocalize with NR2A or NR2B in naive cultures (Fig. 2, B and C). Treatment with lithium (5 mM) for 4 h increased the number of PSD95-GFP puncta from 108 ± 3 ($n = 5$) in naive cultures to 230 ± 19 ($n = 6$). Despite the 113% increase in the number of puncta in lithium-treated cultures, the colocalization of PSD95-GFP puncta with NR2A or NR2B immunoreactivity was similar, with $71 \pm 2\%$ ($n = 6$) of PSD95-GFP puncta colabeling for NR2A or NR2B. Therefore, new PSD95-GFP puncta formed during treatment with lithium colocalize with sites of NR2A or NR2B immunoreactivity.

We also determined whether functional presynaptic terminals were apposed to the newly formed PSDs. Functional neurotransmitter release sites were labeled with FM4–64FX. Using a protocol to stimulate vesicle release and recycling, FM4–64FX loaded into synaptic vesicles during endocytosis. The cells were fixed, and the relative locations of PSD95-GFP and FM4–64FX puncta were determined by image processing (Fig. 3). In naive cultures, $68 \pm 2\%$ ($n = 7$) of PSD95-GFP puncta colocalize with FM4–64FX. In cultures treated with lithium (5 mM), $70 \pm 3\%$ ($n = 11$) of PSD95-GFP puncta colocalize with FM4–64FX. Because a similar percentage of PSD95-GFP puncta colabeled with presynaptic release sites, we conclude that the new puncta represent functional synapses and are comparable with those in naive cells.

Lithium-Induced Synapse Formation Requires Protein Synthesis and Synaptic Transmission. We next determined whether lithium-induced synapse formation required de novo synthesis of protein. To examine this possibility, we pretreated the culture with the protein synthesis inhibitor cycloheximide (10 μM) (Fig. 4, A and B). Blocking translation prevented lithium-induced synapse formation. In the presence of cycloheximide, lithium induced a $33 \pm 10\%$ ($n = 5$) change in the number of PSD95-GFP puncta, compared with a $143 \pm 16\%$ ($n = 10$) increase in untreated cells. Cycloheximide also prevented the small increase in fluorescent puncta seen in nonstimulated cells ($-5 \pm 10\%$, $n = 7$). Thus, protein synthesis is required for the maintenance and up-regulation of PSDs.

Synaptic activity stabilizes neuronal connections during synaptogenesis (Muller and Nikonenko, 2003). We examined whether lithium-induced synapse formation required activation of glutamate receptors (Fig. 4B). Pretreatment with the NMDA receptor antagonist MK801 (10 μM) significantly inhibited lithium-induced synapse formation ($31 \pm 11\%$, $n = 8$). Likewise, pretreatment with the α-amino-3-hydroxy-5-methyl-4-isoxazolepropionic acid/kainate receptor antagonist CNQX (10 μM) also inhibited the formation of new synapses ($50 \pm 14\%$, $n = 4$). Thus, new synaptic sites

induced by lithium treatment require postsynaptic activation for stable expression.

Inositol Depletion Mediates the Effects of Lithium on Synapse Formation. We next determined the mechanism of lithium-induced synapse formation. Many of the cellular effects of lithium have been ascribed to either inhibition of GSK-3β, which is abundantly expressed in the brain (Wexler et al., 2008) or via a direct inhibition of inositol monophosphatase and inositol polyphosphatase, which recycle inositol from inositol phosphates (Berridge, 1989) (Fig. 5A). If GSK-3β is the molecular target for lithium-induced synapse formation, then inhibition of this enzyme by other drugs should mimic the effects of lithium on PSD95-GFP puncta. Application of the cell-permeant GSK-3β inhibitory peptide N-myristol-GKEAPPAPPQS(p)P (L803-mts; 40 μM) did not induce the formation of new synapses (60 $\pm$ 13%, n = 7) (Fig. 5B). In control Western blot experiments (Supplementary Fig. 1), L803-mts (40 μM, 4 h) increased β-catenin levels, a

consequence of GSK3-β inhibition. Other GSK-3β inhibitors such as SB216763 and SB415286 fluoresced at the wavelengths used in this assay precluding their use. The GSK-3β inhibitor 4-benzyl-2-methyl-1,2,4-thiadiazolidine-3,5-dione was toxic at the micromolar concentrations reported to inhibit GSK-3β. In the presence of 4-benzyl-2-methyl-1,2,4-thiadiazolidine-3,5-dione, cells either detached from the coverslip or failed to retain DsRed2 in the cytoplasm (n = 3). Because GSK-3β was not evidently the site of action for lithium-induced synapse formation, we turned our attention to the phosphoinositide cascade.

Inhibition of inositol phosphatases results in the depletion of the free inositol required for phosphoinositide-mediated intracellular signaling cascades (Berridge, 1989). If inhibition of inositol phosphatases was the site of lithium action, then providing exogenous *myo*-inositol should prevent lithium-induced changes in PSDs. *Myo*-inositol (1 mM) inhibited lithium-induced synapse formation (60 $\pm$ 7%, n = 8), sug-
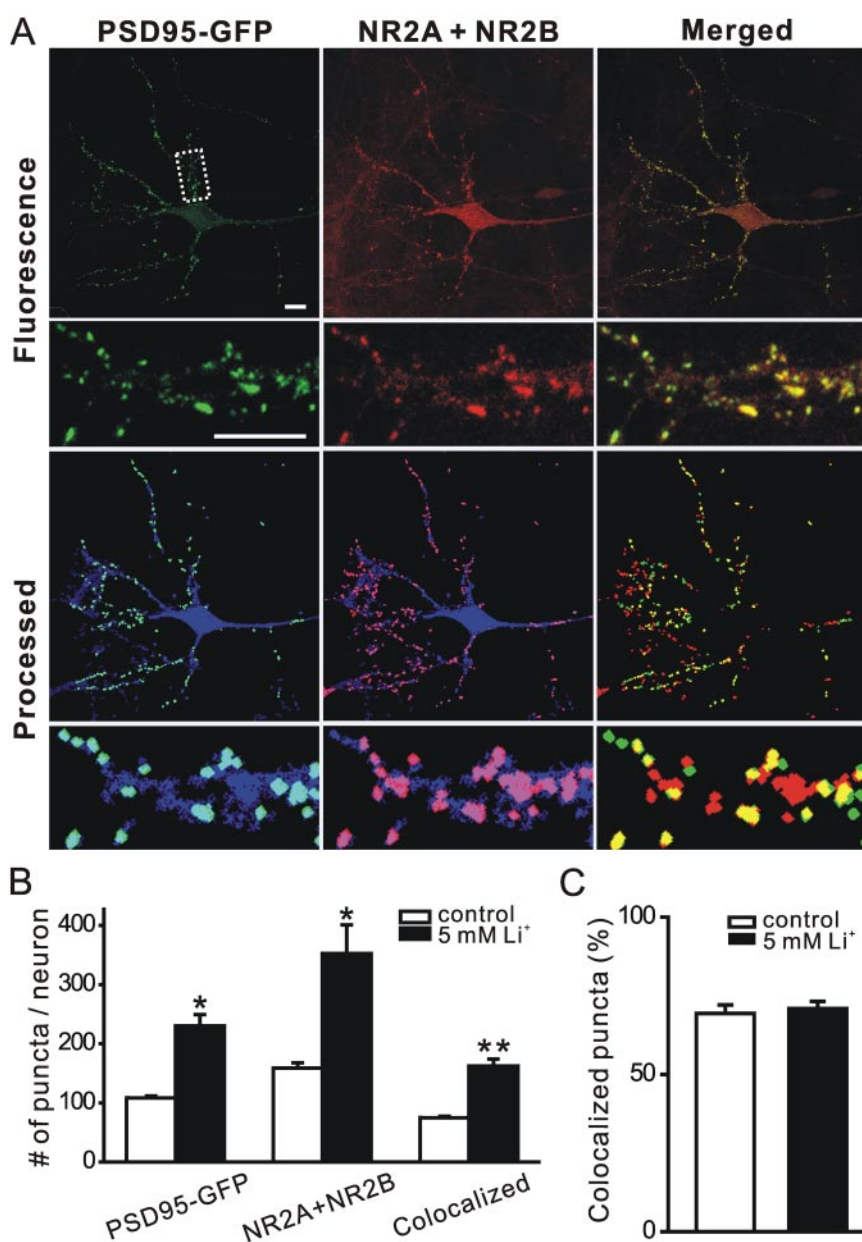

Fig. 2. New PSD95-GFP puncta induced by lithium represent synaptic sites. A, confocal micrographs display NR2A and NR2B (red) immunoreactivity and PSD95-GFP fluorescence (green). Processed images display puncta within the DsRed2 mask (blue). The image-processing algorithm described under *Materials and Methods* was used to identify NR2 immunoreactive puncta and PSD95-GFP puncta. Merged images display overlapping puncta (yellow). The insets are enlarged images of the boxed region. Note that NR2A and NR2B immunoreactivity includes nontransfected cells in the field. Scale bar, 10 μm. B, quantification of PSD95-GFP puncta, NR2A, and NR2B, and PSD95-GFP puncta colocalized with NR2A and NR2B for neurons under control conditions ($\square$) and after treatment with 5 mM lithium ($\blacksquare$). Data are presented as mean $\pm$ S.E.M. *, p < 0.05, **, p < 0.01, lithium-treated compared with control. C, bar graph shows the percentage of PSD95-GFP puncta colocalized with NR2A and NR2B under control conditions ($\square$) and after 4-h treatment with 5 mM lithium ($\blacksquare$). Data are presented as mean $\pm$ S.E.M.

gesting that depletion of inositol contributed to the increase in synaptic connections (Fig. 5B).

Myo-inositol is the substrate for synthesis of the membrane lipid PtdIns, which is phosphorylated on the inositol carbon ring to form PtdIns phosphates. We used a pharmacological approach to identify the key lipid molecules mediating the effects of lithium. Wortmannin inhibits selectively PtdIns 3-kinase (PI3K) at the relatively low concentration of 100 nM. Pretreatment with 100 nM wortmannin did not affect PSD95-GFP puncta directly or inhibit lithium-induced synapse formation (Fig. 5C). Thus, depletion of PtdIns(3,4)P_2 and PtdIns(3,4,5)P_3 were not mediating the effects of lithium on synapse formation. PtdIns(4,5)P_2 is hydrolyzed by phospholipase C (PLC) to release inositol triphosphate and diacyl glycerol. We next determined whether inhibition of PLC or protein kinase C (PKC) activity mimicked the effects of lithium on synapse formation. Treatment with the PLC inhibitor U73122 (1 μM) or the PKC inhibitors Gö6976 or Ro-31-8220 (100 nM) did not affect the number of PSD95 puncta (Fig. 5C). These results suggested that depletion of phosphoinositides upstream of PI3K and PLC such as PtdIns(4)P or PtdIns(4,5)P_2 might mediate the effects of lithium. At the relatively high concentration of 10 μM, wortmannin inhibits PtdIns 4-kinase. Application of wortmannin (10 μM) to the culture increased the number of PSD95-GFP puncta by 139 $\pm$ 15% (n = 8), thus mimicking the actions of lithium (Fig. 5C).

If depletion of PtdIns(4)P or PtdIns(4,5)P_2 was mediating the effects of lithium and 10 μM wortmannin, then adding exogenous PtdIns(4)P or PtdIns(4,5)P_2 should prevent new synapse formation. These hydrophobic molecules can be added to cells using a lipid-based carrier system (Fig. 5D). Application of PtdIns(4)P via the Shuttle PIP system to hippocampal cultures before treatment with wortmannin abolished wortmannin-induced synapse formation (53 $\pm$ 13%, n = 5). Exogenous PtdIns(4)P also prevented lithium-induced synapse formation (55 $\pm$ 19%, n = 5). PtdIns(4)P alone did not affect the number of synapses (44 $\pm$ 10%, n = 5). PtdIns(4,5)P_2 in combination with its carrier was toxic to hippocampal neurons, precluding reconstitution experiments with this phospholipid. Thus, we could not determine whether depletion of PtdIns(4,5)P_2 contributes to the effects of lithium on synapse formation. Depletion of PtdIns(4,5)P_2 in some systems signals to effectors such as KCNQ channels. However, direct inhibition of KCNQ channels with XE991
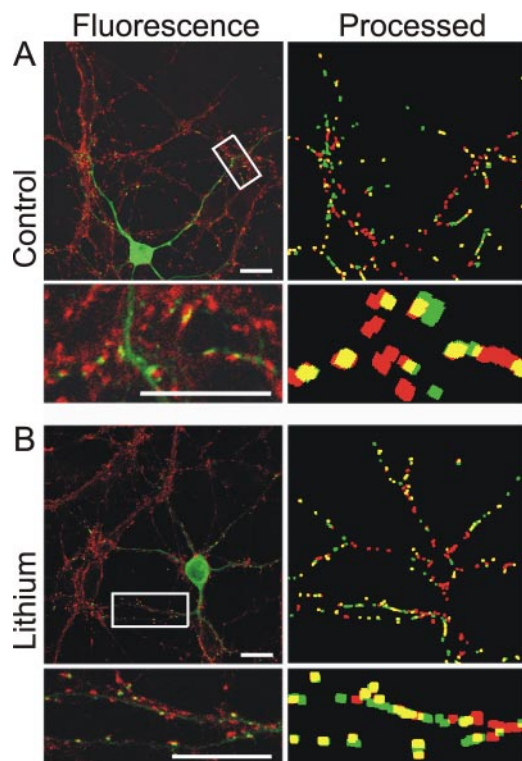

Fig. 3. New PSD95-GFP puncta induced by lithium are in close apposition to neurotransmitter release sites. Fluorescence and processed images from naive (control) (A) and lithium-treated (5 mM, 4 h) (B) cells show PSD95-GFP (green) and FM4–64FX-labeled functional release sites (red) and overlapping puncta (yellow). FM4–64FX was loaded into synaptic vesicles of neurons expressing PSD95-GFP by depolarization-induced (50 mM K$^+$) vesicular recycling, fixed, and then imaged with confocal microscopy. Note that FM4–64FX labels all cells in the field, whereas PSD95-GFP puncta are only present in the transfected cell. Scale bar, 10 μm.
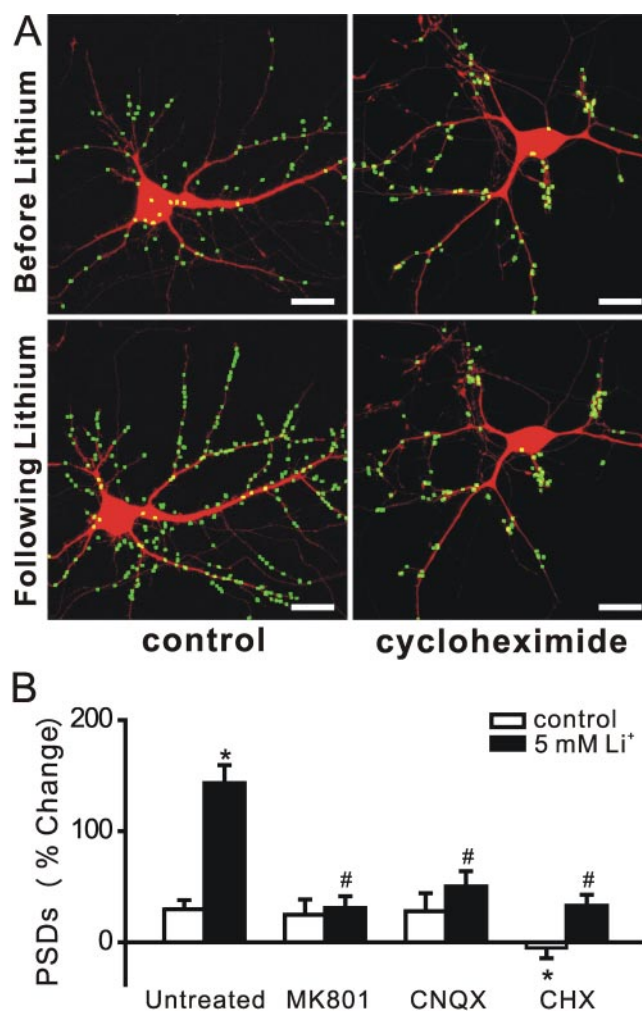

Fig. 4. Synapse formation induced by lithium requires translation and neurotransmission. A, processed images acquired before and after 4-h treatment with 5 mM lithium in the absence (control) and presence of 10 μM cycloheximide display labeled PSDs superimposed on DsRed2 fluorescence. Scale bar, 10 μm. B, bar graph shows change in the number of PSDs after 4-h treatment with vehicle (control, □) or 5 mM lithium (■) in the absence (untreated) or presence of 10 μM MK801, 10 μM CNQX, or 10 μM cycloheximide (CHX) as indicated. Data are presented as mean $\pm$ S.E.M. ∗, p < 0.01 compared with untreated control; #, p < 0.01 compared with lithium-induced response in the absence of drug (untreated), ANOVA with Bonferroni's multiple comparison test.

failed to induce new synapse formation ($46 \pm 15\%$, $n = 6$). (Fig. 5E).

Presynaptic Inhibition Abolishes Lithium-Induced Synapse Formation. Previous work has indicated that new presynaptic terminals form after treatment with lithium (Hall et al., 2000). We used an imaging-based approach similar to that used to quantify PSDs to count synaptophysin-GFP puncta. Consistent with previous immunocytochemistry-based approaches, lithium increased the number of synaptophysin-GFP puncta by $126 \pm 20\%$ ($n = 7$) (Fig. 6A). Because formation of the presynaptic terminal typically precedes formation of the PSD (Friedman et al., 2000), and because activation of postsynaptic glutamate receptors was required for lithium-induced synapse formation (Fig. 4B), we examined the possibility that pharmacological modulation of glutamate release could modulate the effects of lithium on synapses. As shown in Fig. 6B, blocking presynaptic voltage-gated Ca^{2+} channels with the N-type channel blocker ω-conotoxin GVIA or the P,Q-type channel blocker ω-agatoxin IVA prevented lithium-induced synapse formation. Activating the CB1 cannabinoid receptor inhibits presynaptic Ca^{2+} channels and reduces neurotransmitter release (Shen et al., 1996). The cannabinoid receptor agonist Win 55,212-2 also prevented lithium-induced synapse formation ($29 \pm 16\%$, $n = 7$).

Discussion

Lithium induced the formation of new synapses between hippocampal neurons. This observation is consistent with the lithium-induced increase in neuropil in bipolar patients (Chen et al., 2000; Sassi et al., 2002), lithium-induced axonal sprouting (Hall et al., 2000), the mislocalization of synapses in lithium-treated animals (Tanizawa et al., 2006), and increases in the amplitude of excitatory postsynaptic potentials after lithium treatment (Shim et al., 2007). The increase in synapses resulted from lithium-induced depletion of inositol and required excitatory synaptic activity and protein synthesis. Although IMPase and IPPase are established targets for lithium, inositol depletion has not previously been shown to increase the formation of synapses. This mechanism of synapse regulation may underlie some of the clinical effects of lithium and suggests novel mechanisms for regulating synaptic function.

We used an imaging-based assay to detect changes in the number of PSDs after drug treatment. Previous validation experiments confirmed that PSD95-GFP fluorescent puncta represent functional synaptic sites (Waataja et al., 2008). We confirmed in this study that the new puncta that formed during lithium treatment contained NR2-immunoreactivity and were apposed to functional sites of neurotransmitter
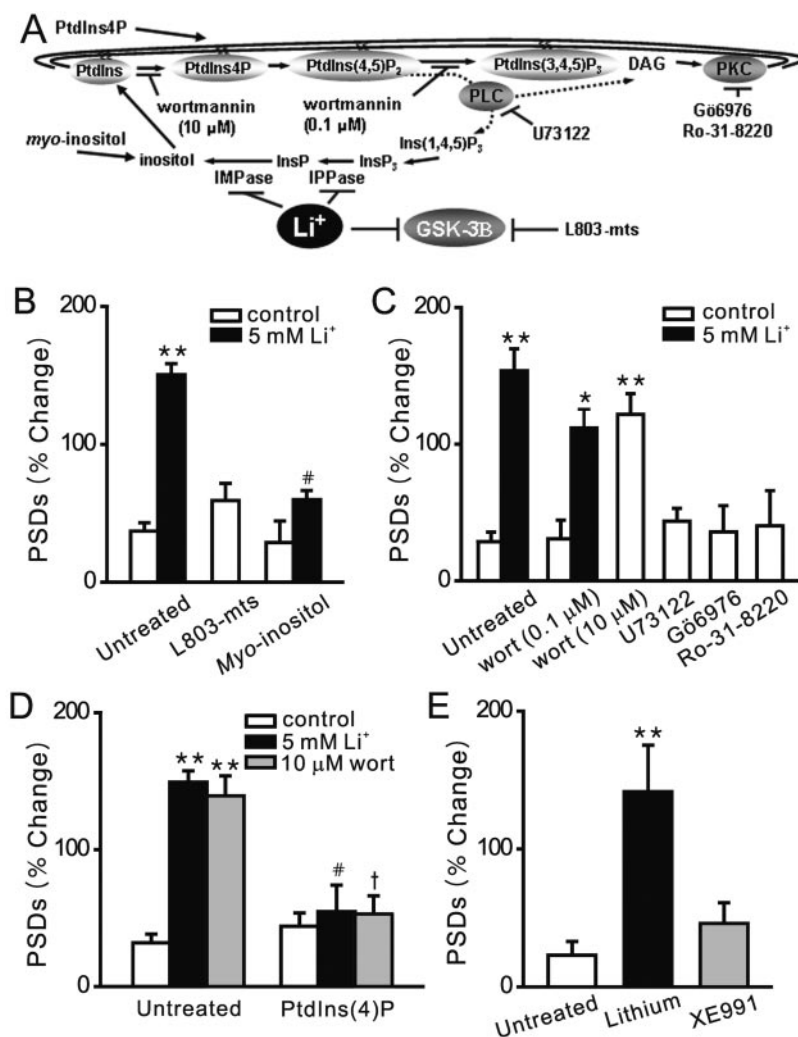

Fig. 5. Inositol depletion mediates the effects of lithium on synapse formation. A, the phosphoinositide cascade. B, bar graph summarizes the effects of GSK-3β inhibitor L803-mts and exogenous *myo*-inositol on changes in PSD95-GFP puncta (PSDs) after 4-h treatment under control (□) or stimulated (5 mM Li$^+$, ■) conditions. Pretreatment with 1 mM *myo*-inositol prevented the formation of new PSDs. C, bar graph summarizes the effects of pharmacological modulation of the PtdIns cascade on synapse formation in the absence (□) or presence of 5 mM lithium (■). Wortmannin [10 μM; wort (10 μM)] but not 100 nM wortmannin [wort(0.1 μM)] induced new synapse formation. Inhibition of PLC with 1 μM U73122 or inhibition of PKC with either 100 nM Gö6976 or 100 nM Ro-31-8220 did not affect the number of PSD95-GFP puncta. D, bar graph summarizes the effects on exogenous PtdIns(4)P on the number of PSD95-GFP puncta under control conditions (□) or during treatment with 5 mM lithium (■) or 10 μM wortmannin (▤). PtdIns(4)P was delivered via the shuttle PIP system as described under *Materials and Methods*. E, bar graph summarizes the effects of 10 μM XE991 on the number of PSD95-GFP puncta under control conditions (▤). Data are mean $\pm$ S.E.M. ∗, $p < 0.05$, ∗∗, $p < 0.01$ relative to untreated control; #, $p < 0.01$ relative to lithium-induced response in the absence of other treatments (untreated); †, $p < 0.01$ relative to wortmannin-induced response in the absence of other treatments (untreated); ANOVA with Bonferroni post test.

release, consistent with the assembly of functional synapses. We also showed that lithium induced a corresponding increase in fluorescent puncta formed by the presynaptic marker synaptophysin-GFP. Image processing of PSD95-GFP puncta before and after treatment enabled quantitative analysis suitable for mechanistic studies. A modest increase in the number of synapses under control conditions was observed previously (Kim et al., 2008). Unlike the increase induced by lithium, glutamate receptor antagonists did not inhibit it, although protein synthesis was required. Media exchange at the start of the experiment initiated the increase under control conditions. Primary cultures are extremely sensitive to medium composition and physical agitation (Kretz et al., 2007). We note that the increase in the number of synapses under control conditions is small relative to the large and sustained increase induced by lithium.

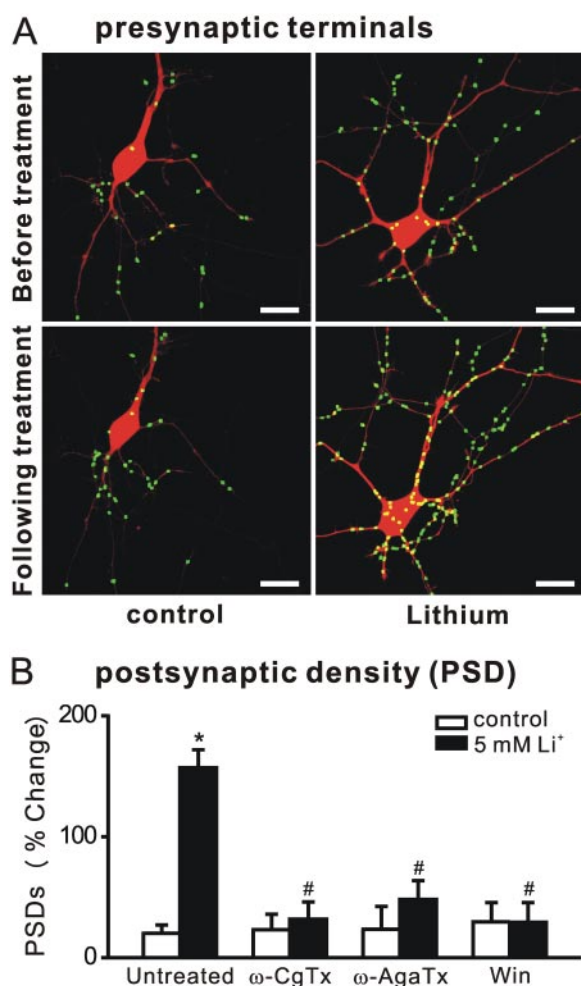The conclusion that lithium induced the formation of new

Fig. 6. Presynaptic regulation of lithium-induced synapse formation. A, processed images acquired before and after 4-h treatment with 5 mM lithium display fluorescent puncta formed from the expression of synaptophysin fused to GFP superimposed on DsRed2 fluorescence. Scale bar, 10 μm. Note that many hippocampal neurons in culture form autapses. B, relative change in the number of PSDs (average percentage change from initial counts) after 4-h treatment in the presence of the presynaptic Ca^{2+}-channel blockers 1 μM ω-conotoxin GVIA (ω-CgTx) and 1 μM ω-agatoxin IVA (ω-AgaTx) or the cannabinoid receptor agonist 100 nM Win 55,212-2 (Win). Data are presented as mean $\pm$ S.E.M. *, $p < 0.01$ compared with untreated control; #, $p < 0.01$ compared with lithium-induced response in the absence of drug (untreated), ANOVA with Bonferroni post test.

synapses by inhibition of IMPase and IPPase is supported by several findings described here. L803-mts was shown to effectively inhibit GSK-3β in hippocampal cultures, yet it failed to induce the formation of new synapses. On the other hand, the EC_{50} value of 1.0 ± 0.6 mM for lithium-induced synapse formation is in good agreement with IC_{50} values of 0.3 to 1.5 mM reported for lithium inhibition of IMPase (Atack et al., 1994). That lithium induced new synapse formation by acting on the PtdIns cascade was indicated by the prevention of new synapse formation when *myo*-inositol or PtdIns(4)P was supplied and by the induction of new synapses that resulted from inhibition of PtdIns 4-kinase. Thus, lithium-induced synapse formation proceeds via a mechanism distinct from the proliferative and neuroprotective actions of lithium, which seem to be primarily mediated via inhibition of GSK-3β (Jope and Bijur, 2002). In rat hippocampal cultures, lithium inhibition of GSK-3β reduced τ phosphorylation and inhibited neurite outgrowth, a result that would seem unlikely to increase the formation of synapses (Takahashi et al., 1999). In contrast, other studies suggest that lithium, like WNT-7a, might induce synapse formation by reducing GSK-3β activity to elicit a subsequent increase in axonal remodeling (Hall et al., 2000). Inositol depletion has not previously been reported to induce the formation of synapses. The reconstitution experiments indicate that new synapses formed as a result of depleted PtdIns(4)P and possibly PtdIns(4,5)P_2. Loss of inositol lipids has been attributed to defects in membrane trafficking and secretion (Wenk and De Camilli, 2004), but this seems unlikely to increase synapse formation. Recent studies found that depletion of PtdIns(4,5)P_2 by receptor-induced activation of PLC is a physiological mechanism for inhibition of KCNQ K^+ channels (Suh et al., 2004). However, direct inhibition of KCNQ channels with XE991 failed to induce new synapse formation. The idea that depletion of PtdIns(4,5)P_2 leads to a direct change in a signaling molecule is consistent with our pharmacological studies that ruled out a role for subsequent processing of PtdIns(4,5)P_2 by PI3K or PLC.

PtdIns(4,5)P_2 balance is required for normal neurotransmission, and the gene encoding the PtdIns(4,5)P_2 phosphatase synaptojanin 1 (*SYNJ1*) has been implicated in bipolar disorder (Halstead et al., 2005). Thus, it is reasonable to expect that depletion of PtdInsP with a corresponding decrease in PtdIns(4,5)P_2 might alter synapse formation. PtdIns(4,5)P_2 regulates focal adhesion kinase (FAK) by releasing an autoinhibitory interaction that allows FAK to adopt its active conformation (Cai et al., 2008). FAK inhibits the formation of axonal terminals, and thus, inactivation of FAK leads to increased synapse formation (Rico et al., 2004). Depletion of PtdIns(4,5)P_2 with subsequent inhibition of FAK is a plausible mechanism by which lithium might trigger new synapse formation. Interestingly, the subcellular distribution of PtdIns 4- and 5-kinases suggest that localized changes in PtdIns(4,5)P_2 might play important signaling roles (Doughman et al., 2003). Thus, lithium might produce localized rather than widespread depletion of inositol to exert its effects.

Synaptic activity was required for the effects of lithium. Blocking postsynaptic NMDA receptors or presynaptic calcium channels prevented the formation of new synapses, although KCNQ channel-mediated changes in excitability were not sufficient to induce the formation of new synapses.

Interestingly, intense activation of NMDA receptors either by direct application of agonist or from exposure to an epileptic pattern of excitatory synaptic activity caused synapse loss (Kim et al., 2008; Waataja et al., 2008). Thus, the intensity of synaptic activity can influence the polarity of changes in synaptic number, consistent with similar results regulating long-term synaptic plasticity and activity-dependent development of neural circuitry (Stanton, 1996). Cannabinoids act presynaptically to inhibit neurotransmitter release (Shen et al., 1996). Activation of cannabinoid receptors prevented lithium-induced synapse formation, highlighting the necessity for glutamate release and suggesting a potential drug interaction. Many bipolar patients are substance abusers and frequently use marijuana (Cassidy et al., 2001).

New synapse formation required the synthesis of new proteins. Yet lithium induced a significant increase in the number of synapses within 4 h. The rapid development of new synapses in remote regions of the dendrite suggests that translation may have occurred in the dendrite using local mRNA (Schuman, 1999). Thus, the dendrites seem to be poised for the rapid production of new proteins needed to form new synapses, suggesting that lithium may recruit an existing mechanism established for synaptic development or plasticity.

The rapid increase in synapses induced by lithium seems to indicate that new synapse formation does not underlie the stabilization of mood in bipolar patients because the therapeutic effects of lithium require 1 to 2 weeks to develop (Baldessarini and Tarazi, 2006). However, it has been noted that synaptic spines in culture change more rapidly than spines imaged in vivo (Grutzendler et al., 2002), so the culture model could be accelerated relative to the intact brain. In addition, the rate and magnitude of lithium-induced changes in inositol levels differ between species and in vivo and in vitro models (Belmaker et al., 1996). Thus, PtdIns(4,5)P depletion may require more time in humans than in the model used here. Alternatively, new synapse formation may underlie some of the untoward effects of lithium. Intracerebral injection of pilocarpine and lithium in combination is a widely used method to kindle seizures (Honchar et al., 1983). Interestingly, axonal sprouting in the hippocampus occurs within hours of inducing status epilepticus by this method (Mello et al., 1993). Perhaps the synapse formation we describe here is related to the adverse effects of lithium, which include convulsions (Baldessarini and Tarazi, 2006).

In summary, we have shown that lithium-induced inositol depletion increases the formation of new synapses. These findings suggest a potential physiological role for changes in PtdInsP levels to regulate synaptic number. These results also raise interesting questions concerning how changes in the number of synaptic contacts relate to mood and epilepsy.

Acknowledgments

References

Allison JH and Stewart MA (1971) Reduced brain inositol in lithium-treated rats. *Nature New Biol* **233:**267–268.
Atack JR, Prior AM, Fletcher SR, Quirk K, McKernan R, and Ragan CI (1994) Effects of L-690,488, a prodrug of the bisphosphonate inositol monophosphatase inhibitor L-690,330, on phosphatidylinositol cycle markers. *J Pharmacol Exp Ther* **270:**70–76.
Baldessarini RJ and Tarazi FI (2006) Pharmacotherapy of psychosis and mania, in *Goodman and Gilman's The Pharmacological Basis of Therapeutics*, 11th ed. (Brunton LL, Lazo JS, and Parker KL eds) pp 461–500, McGraw-Hill, New York.
Belmaker RH, Bersudsky Y, Agam G, Levine J, and Kofman O (1996) How does lithium work on manic depression? Clinical and psychological correlates of the inositol theory. *Annu Rev Med* **47:**47–56.
Berridge MJ (1989) The Albert Lasker Medical Awards. Inositol trisphosphate, calcium, lithium, and cell signaling. *JAMA* **262:**1834–1841.
Cai X, Lietha D, Ceccarelli DF, Karginov AV, Rajfur Z, Jacobson K, Hahn KM, Eck MJ, and Schaller MD (2008) Spatial and temporal regulation of focal adhesion kinase activity in living cells. *Mol Cell Biol* **28:**201–214.
Cassidy F, Ahearn EP, and Carroll BJ (2001) Substance abuse in bipolar disorder. *Bipolar Disord* **3:**181–188.
Chen G, Rajkowska G, Du F, Seraji-Bozorgzad N, and Manji HK (2000) Enhancement of hippocampal neurogenesis by lithium. *J Neurochem* **75:**1729–1734.
Chuang DM and Manji HK (2007) In search of the holy grail for the treatment of neurodegenerative disorders: has a simple cation been overlooked? *Biol Psychiatry* **62:**4–6.
Doughman RL, Firestone AJ, and Anderson RA (2003) Phosphatidylinositol phosphate kinases put PI4,5P₂ in its place. *J Membr Biol* **194:**77–89.
Friedman HV, Bresler T, Garner CC, and Ziv NE (2000) Assembly of new individual excitatory synapses: time course and temporal order of synaptic molecule recruitment. *Neuron* **27:**57–69.
Gould TD, Quiroz JA, Singh J, Zarate CA, and Manji HK (2004) Emerging experimental therapeutics for bipolar disorder: insights from the molecular and cellular actions of current mood stabilizers. *Mol Psychiatry* **9:**734–755.
Grutzendler J, Kasthuri N, and Gan WB (2002) Long-term dendritic spine stability in the adult cortex. *Nature* **420:**812–816.
Hall AC, Lucas FR, and Salinas PC (2000) Axonal remodeling and synaptic differentiation in the cerebellum is regulated by WNT-7a signaling. *Cell* **100:**525–535.
Halstead JR, Jalink K, and Divecha N (2005) An emerging role for PtdIns(4,5)P2-mediated signalling in human disease. *Trends Pharmacol Sci* **26:**654–660.
Honchar MP, Olney JW, and Sherman WR (1983) Systemic cholinergic agents induce seizures and brain damage in lithium-treated rats. *Science* **220:**323–325.
Jope RS and Bijur GN (2002) Mood stabilizers, glycogen synthase kinase-3beta and cell survival. *Mol Psychiatry* **7 (Suppl 1):**S35–S45.
Kim E and Sheng M (2004) PDZ domain proteins of synapses. *Nat Rev Neurosci* **5:**771–781.
Kim HJ, Waataja JJ, and Thayer SA (2008) Cannabinoids inhibit network-driven synapse loss between hippocampal neurons in culture. *J Pharmacol Exp Ther* **325:**850–858.
Kretz A, Marticke JK, Happold CJ, Schmeer C, and Isenmann S (2007) A primary culture technique of adult retina for regeneration studies on adult CNS neurons. *Nat Protoc* **2:**131–140.
Lovestone S, Davis DR, Webster MT, Kaech S, Brion JP, Matus A, and Anderton BH (1999) Lithium reduces tau phosphorylation: effects in living cells and in neurons at therapeutic concentrations. *Biol Psychiatry* **45:**995–1003.
Mello LE, Cavalheiro EA, Tan AM, Kupfer WR, Pretorius JK, Babb TL, and Finch DM (1993) Circuit mechanisms of seizures in the pilocarpine model of chronic epilepsy: cell loss and mossy fiber sprouting. *Epilepsia* **34:**985–995.
Muller D and Nikonenko I (2003) Dynamic presynaptic varicosities: a role in activity-dependent synaptogenesis. *Trends Neurosci* **26:**573–575.
Okabe S, Kim HD, Miwa A, Kuriu T, and Okado H (1999) Continual remodeling of postsynaptic density and its regulation by synaptic activity. *Nature Neurosci* **2:**804–811.
Okabe S, Miwa A, and Okado H (2001) Spine formation and correlated assembly of presynaptic and postsynaptic molecules. *J Neurosci* **21:**6105–6114.
Ozaki S, DeWald DB, Shope JC, Chen J, and Prestwich GD (2000) Intracellular delivery of phosphoinositides and inositol phosphates using polyamine carriers. *Proc Natl Acad Sci U S A* **97:**11286–11291.
Rico B, Beggs HE, Schahin-Reed D, Kimes N, Schmidt A, and Reichardt LF (2004) Control of axonal branching and synapse formation by focal adhesion kinase. *Nat Neurosci* **7:**1059–1069.
Sassi RB, Nicoletti M, Brambilla P, Mallinger AG, Frank E, Kupfer DJ, Keshavan MS, and Soares JC (2002) Increased gray matter volume in lithium-treated bipolar disorder patients. *Neurosci Lett* **329:**243–245.
Schloesser RJ, Huang J, Klein PS, and Manji HK (2008) Cellular plasticity cascades in the pathophysiology and treatment of bipolar disorder. *Neuropsychopharmacology* **33:**110–133.
Schuman EM (1999) mRNA trafficking and local protein synthesis at the synapse. *Neuron* **23:**645–648.
Shen M, Piser TM, Seybold VS, and Thayer SA (1996) Cannabinoid receptor agonists inhibit glutamatergic synaptic transmission in rat hippocampal cultures. *J Neurosci* **16:**4322–4334, .
Shim SS, Hammonds MD, Ganocy SJ, and Calabrese JR (2007) Effects of sub-chronic lithium treatment on synaptic plasticity in the dentate gyrus of rat hippocampal slices. *Prog Neuropsychopharmacol Biol Psychiatry* **31:**343–347.
Stanton PK (1996) LTD, LTP, and the sliding threshold for long-term synaptic plasticity. *Hippocampus* **6:**35–42.
Suh BC, Horowitz LF, Hirdes W, Mackie K, and Hille B (2004) Regulation of KCNQ2/KCNQ3 current by G protein cycling: the kinetics of receptor-mediated signaling by Gq. *J Gen Physiol* **123:**663–683.
Takahashi M, Yasutake K, and Tomizawa K (1999) Lithium inhibits neurite growth and tau protein kinase I/glycogen synthase kinase-3beta-dependent phosphorylation of juvenile tau in cultured hippocampal neurons. *J Neurochem* **73:**2073–2083.
Tanizawa Y, Kuhara A, Inada H, Kodama E, Mizuno T, and Mori I (2006) Inositol

monophosphatase regulates localization of synaptic components and behavior in the mature nervous system of C. elegans. *Genes Dev* **20:**3296–3310.

Waataja JJ, Kim HJ, Roloff AM, and Thayer SA (2008) Excitotoxic loss of postsynaptic sites is distinct temporally and mechanistically from neuronal death. *J Neurochem* **104:**364–375.

Wenk MR and De Camilli P (2004) Protein-lipid interactions and phosphoinositide metabolism in membrane traffic: insights from vesicle recycling in nerve terminals. *Proc Natl Acad Sci U S A* **101:**8262–8269.

Wexler EM, Geschwind DH, and Palmer TD (2008) Lithium regulates adult hippocampal progenitor development through canonical Wnt pathway activation. *Mol Psychiatry* **13:**285–292.

Williams RS, Cheng L, Mudge AW, and Harwood AJ (2002) A common mechanism of action for three mood-stabilizing drugs. *Nature* **417:**292–295.

Address correspondence to: Dr. Stanley A. Thayer, Department of Pharmacology, University of Minnesota, 6–120 Jackson Hall, 321 Church Street SE, Minneapolis, MN 55455. E-mail: sathayer@umn.edu